

DETERMINATION OF SOME PHYSICOCHEMICAL PROPERTIES OF A HEXYLAMINE TREATED SODIUM BENTONITE

M. ÖNAL

Department of Chemistry, Faculty of Sciences, Ankara University, Ankara, TURKEY

(Received May. 1, 2002; Accepted June 11, 2002)

ABSTRACT

A high purity sodium montmorillonite was obtained by the enrichment of a bentonite (RT) taken from Reşadiye (Tokat / Turkey) region and its hexylamine adsorbed form was prepared by the adsorption of hexylamine (HA) from its aqueous solution. The NaM-HA system was investigated by X-ray diffraction (XRD), Fourier transform infrared spectroscopy (FTIR), differential thermal analysis (DTA), thermogravimetric analysis (TGA) and the adsorption of nitrogen at 77K techniques. It was determined that the space between the 2:1 layers of NaM of the HA adsorbed form was 0.18 nm larger than that of NaM. It was observed that this increase lead to a 65 % increase in the specific surface area and 120 % increase in the micropore-mesopore volume of NaM.

INTRODUCTION

Smectites are the major clay minerals of bentonites that are used in many application areas^{1,2}. Montmorillonite and minerals like nontronite, saponite, bidellite and hectorite that are derived from montmorillonite by ion exchange are among the smectite group minerals³. Smectites that have three layered (2:1) sheets are formed by the introduction of an alumina or a magnesia layer between two silica layers⁴. The 2:1 layers become negatively charged by the replacement of high valency ions with lower valency ions⁵. Cations such as Na⁺ and Ca²⁺ enter between the 2:1 layers to provide electroneutrality. These cations are called exchangeable cations since they can be exchanged by any sort of inorganic or organic cations. The cation exchange capacity (CEC) is defined as the equivalent amount of exchanged cations in one kilogram of smectites (or in other cases clays or clay minerals). The kinds of the exchangeable cations as well as the magnitude of the CEC effect considerably the physicochemical properties of smectites such as the colloidal, rheological, ion exchange, and adsorptive properties⁶.

The exchangeable cations of smectites can be replaced by inorganic polycations via ion exchange. The calcination of the obtained material produces pillared clays whose distances between their 2:1 layers have been elongated to a certain extent^{7,8}. Pillared clays are used as molecular sieves and catalysts⁹. On the other hand, the replacement of the exchangeable cations by the cations of

alkylammonium, alkydilammonium, and quaternary ammonium salts via ion exchange produces organoclays^{10,11}. Organoclays are used to modify the rheological properties of some organic systems¹².

Smectites have considerably large ion exchange capacities and they have a large ability to adsorb polar inorganic or organic molecules¹³. Because of these properties, they are used as adsorbents in the purification of discharge waters¹⁴, bleaching of edible oils¹⁵ and clarification of various drinks. For the same reasons, they are used as additives in the production of carbonless copy papers, paints, cosmetics, medications, rubber and plastics¹⁶⁻¹⁸. A detailed investigation of the adsorption of organic molecules possessing some functional groups needs to be made in order to be able to increase the application areas of smectites and to define their functions in their application areas. Therefore, the aim of this study was to investigate the physicochemical properties of an organoclay that was obtained by the adsorption of hexylamine from its solution on high purity sodium montmorillonite.

MATERIALS AND METHOD

A high purity sodium-rich bentonite (NaM) that was obtained by the enrichment of a Reşadiye (Tokat / Turkey) bentonite was chosen as the material^{21,22}. In our previous studies²³ it was determined that the particle size distribution of this bentonite was below 2 μm and its cation exchange capacity was 1.08 mol kg⁻¹. The adsorbant, hexylamine (HA), was supplied by Merck Chemical Company. HA whose density is 0.76 g mL⁻¹, melting point is -23 °C, boiling point is 131 °C and ignition temperature is 270 °C is highly soluble in water.

An infinitely stable suspension was prepared by adding slowly 10 g of NaM on 500 mL of distilled water that was being stirred continuously. 1.6 mL of HA was added dropwise onto the continuously stirred solution. The stirring of the system was continued for 2 more hours after precipitation was complete and was filtered under vacuum through a cloth filter. The precipitate was washed with 10 mL of methanol to remove the excess HA to a certain extent. The organoclay that was dried for 2 hours at 50 °C in an oven was labeled as NaM-HA. The same procedure was repeated 10 times and approximately 100 g of NaM-HA was obtained. The prepared NaM-HA sample was stored in a closely stoppered plastic bottle.

The X-ray diffraction patterns of the NaM-HA sample were determined by a Rikagu D-max 2200 X-ray powder diffractometer in which Cu K α rays that had 0.15418 nm wavelength were used. The IR spectra of NaM, HA and NaM-HA samples were determined by a Mattson 1000 FTIR spectrophotometer in the wavenumber interval 400-4000 cm⁻¹ using the KBr disk procedure. The differential thermal analysis (DTA) and thermogravimetric analysis (TGA) curves of the NaM-HA sample were determined by a Netzsch Simultaneous TG-DTA-DTG Instrument Model 429, at a heating rate of 10 K min⁻¹. Calcined kaolinite was used as an inert material. The isotherms of the adsorption and desorption of nitrogen on the NaM-HA sample at 77K were determined by a volumetric adsorption instrument. The

instrument that was fully constructed of pyrex glass was connected to high vacuum²⁴.

RESULTS AND DISCUSSION

XRD Analyses

The XRD patterns of the NaM and NaM-HA samples are shown in Fig.(1). The $d(001)$ values that represent the 2:1 layer thicknesses of the NaM and NaM-HA samples were calculated respectively as 1.13 and 1.31 nm^{25,26}. The fact that the latter layer thickness was 0.18 nm larger than the former one showed that HA molecules had entered between the layers, in other words, an organoclay was formed as a result of the adsorption. The length and thickness of the HA molecule $[\text{CH}_3-(\text{CH}_2)_4-\text{CH}_2-\text{NH}_2]$ were calculated from the bond lengths respectively as 1.13 nm and 0.21 nm. Therefore, it was understood that the HA molecules could only be adsorbed horizontally between the 2:1 smectite layers.

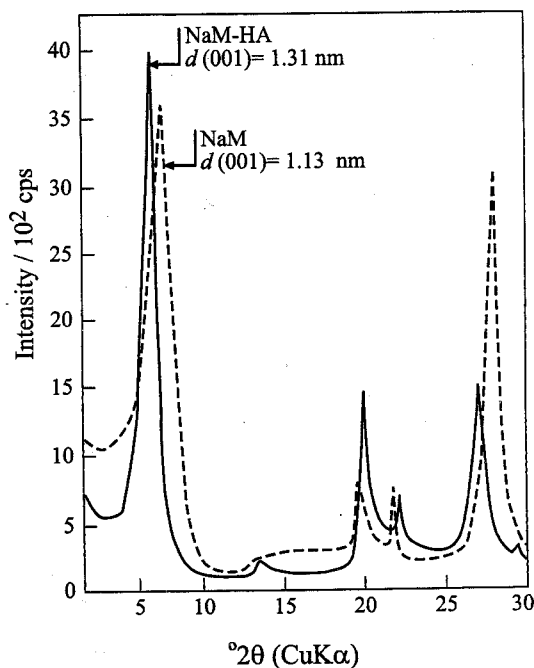


Fig. (1). The XRD patterns of Sodium montmorillonite (NaM) and hexylamine treated sodium montmorillonite (NaM-HA) samples.

FTIR Spectra

FTIR spectra of the NaM, HA and NaM-HA samples are shown in Fig. (2). The bands at lower wave numbered regions of the spectra are due to deformation vibrations of the bonds whereas the bands at high wave numbered regions of the spectra are due to stretching vibrations of the bonds. In the spectrum of NaM the band at 470 cm^{-1} is a Si-O-Si deformation band, the band at 550 cm^{-1} is a Si-O-Al deformation band, the band at 1030 cm^{-1} is a Si-O stretching band, the band at 1634 cm^{-1} is an O-H deformation band of H_2O , the band at 3425 cm^{-1} is an O-H stretching band of H_2O , the band at 3630 cm^{-1} is an O-H stretching band of O-H in the inner surfaces of NaM²⁷. In the spectrum of HA the band at 1100 cm^{-1} is due to C-N stretching, the band at 1380 cm^{-1} is due to planar deformations of C-H bonds in CH_3 , the band at 1450 cm^{-1} is due to planar deformations of C-H bonds in CH_2 , the band at 1600 cm^{-1} is due to planar deformations of N-H bands, the bands at 2870 cm^{-1} and 2960 cm^{-1} are due to C-H bond stretchings, and the band at 3320 cm^{-1} is due to N-H bond stretchings. The fact that the bands contained in both spectra of NaM and HA were present in the spectrum of NaM-HA verified that an organoclay was formed.

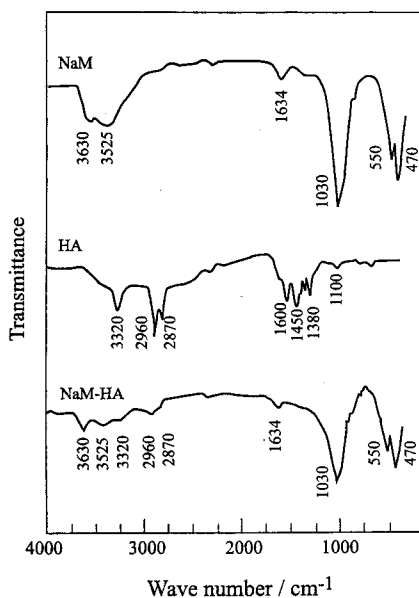


Fig. (2). The FTIR spectra of sodium montmorillonite (NaM), and hexylamine treated sodium montmorillonite (NaM-HA).

Thermal Analyses

The DTA and TGA curves of NaM-HA are presented in Fig. (3). The evaluations³⁰ of the DTA and TGA curves were as follows. The 3.5 % mass loss observed around 200 °C was due to the endothermic loss of water between the 2:1 layers of NaM. The 2.5 % mass loss observed between 200-500 °C was due to the exothermic elimination of HA that was left non-bonded on NaM by burning. The 10 % mass loss between 600-800 °C was due to the endothermic dehydroxylation of NaM and the elimination of the adsorbed HA by burning. The exothermic peak observed between 800-900 °C in the DTA curve showed the recrystallization of NaM that occurred without any mass loss. The total mass loss around 1200 °C was approximately 12 %.

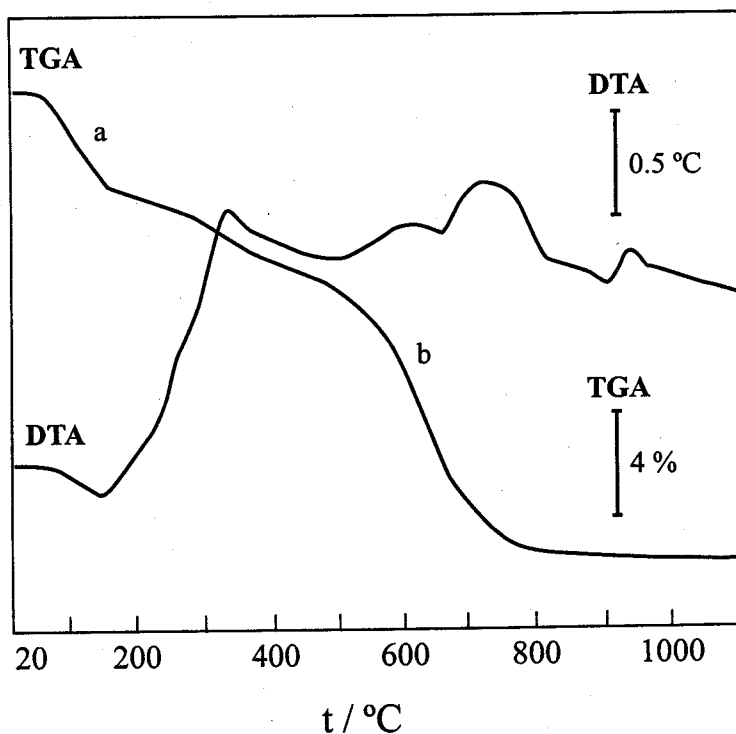


Fig. (3). The DTA and TGA curves of hexylamine treated sodium montmorillonite (NaM-HA).

A decomposition fraction (α) was defined as the ratio of mass loss at any temperature to the total mass loss³¹. The decomposition factors at various temperatures were calculated and plotted as a function of temperature and the α - T curve shown in Fig. (4) was obtained. For thermal transformations of the type, solid (1) solid (2) + gas, such as dehydration, dehydroxylation and calcination the Coats and Redfern (1964) equation³² may be expressed as follows:

$$\ln \left[\frac{-\ln(1-\alpha)}{T^2} \right] = -\frac{E}{RT} + \ln \left[\frac{AR}{\beta E} \left(1 - \frac{2RT}{E} \right) \right] \quad (1)$$

Here, T is the absolute temperature, E is the activation energy, R is the universal gas constant, $\beta = dT/dt$ is the heating rate and $\ln [(AR/\beta E)(1 - 2RT/E)]$ is a nearly constant quantity. The Coats-Redfern straight lines plotted by using the decomposition constants³³ calculated by the TGA data are shown in Fig. (5). Here, the a and b are formed as a result of respectively the dehydration and dehydroxylation of NaM. From the slopes of these curves, the dehydration activation energy and the dehydroxylation activation energy of NaM-HA were calculated respectively as $E_a = 40 \text{ kJ mol}^{-1}$ and $E_b = 51 \text{ kJ mol}^{-1}$. For NaM the above activation energies had been determined respectively as $E_a = 34 \text{ kJ mol}^{-1}$ and $E_b = 67 \text{ kJ mol}^{-1}$ in our previous studies²³. Therefore, it was decided that while the adsorption of HA slowed down the rate of dehydration it accelerated the dehydroxylation.

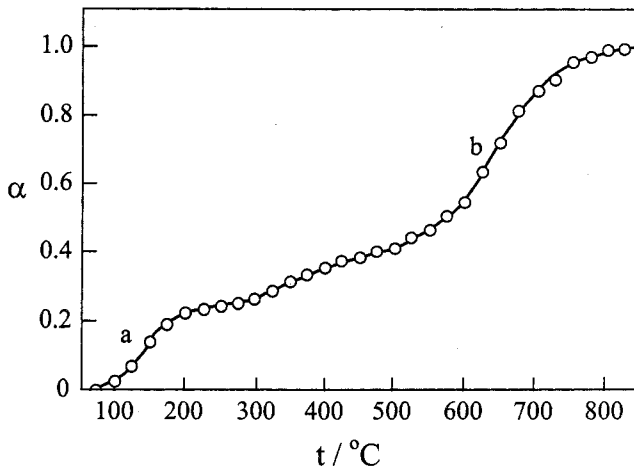


Fig. (4). The variation of the thermal decomposition fraction as a function of temperature for the hexylamine treated sodium montmorillonite (NaM-HA).

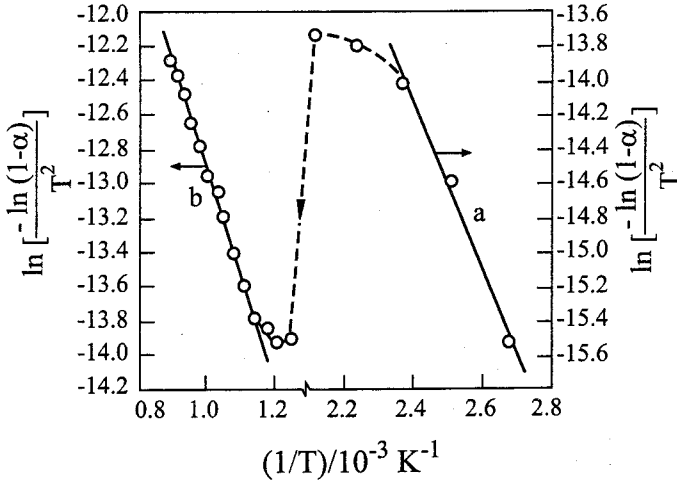


Fig. (5). The Coats-Redfern straight lines of the a)dehydration and b)dehydroxylation of hexylamine treated sodium montmorillonite (NaM-HA).

Surface Area and Porosity

The isotherms of the adsorption and desorption of nitrogen on NaM-HA at 77K are shown in Fig. (6a). Here, p is the equilibrium pressure, p^0 is the condensation pressure of nitrogen at experimental temperature, $p / p^0 = x$ is the relative equilibrium pressure and n is the adsorption capacity that represents the amount of nitrogen adsorbed on one gram of sample (mol g^{-1}). The adsorption capacities were determined in the relative equilibrium pressure interval, $0.05 < x < 0.35$, and they were used to plot the $[x / n(1-x) - x]$ graph according to the following Brunauer, Emmett and Teller (BET) equation³³.

$$x / n(1-x) = 1 / n_m c + [(c-1) / n_m c] x \tag{2}$$

Here, n_m is the monomolecular adsorption capacity and c is a constant. The obtained straight line is shown in Fig. (6b). From the simultaneous solutions of the equations obtained from the slopes and intercepts on the vertical axis of the BET straight line, n_m was calculated as 7.168×10^{-4} and c was calculated as 31.

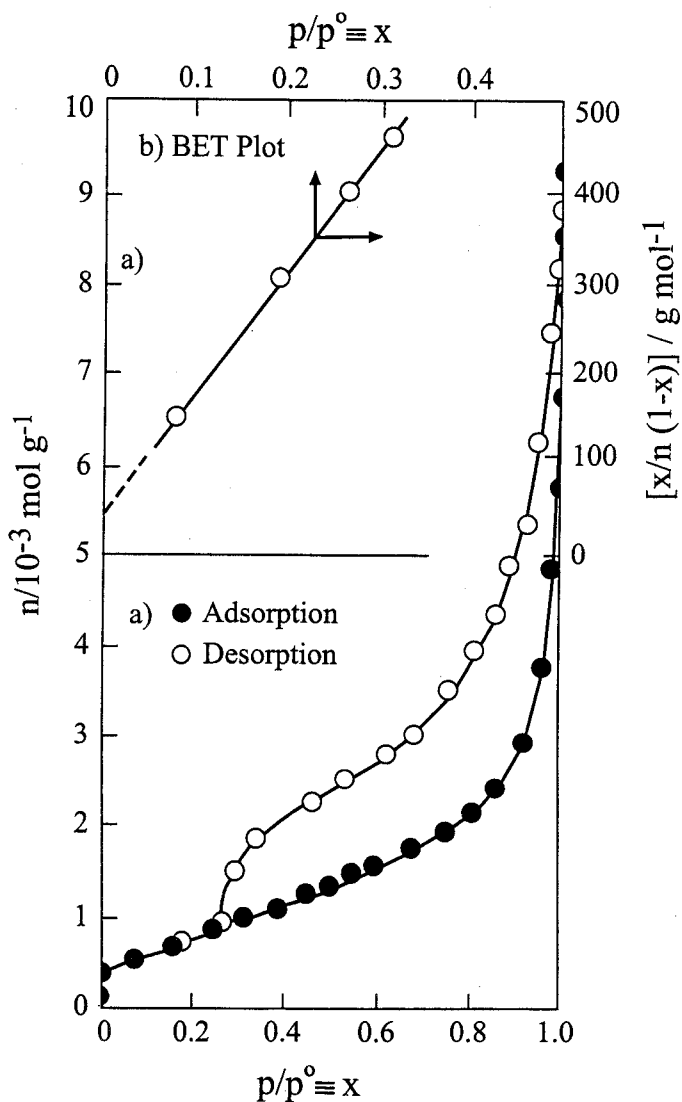


Fig. (6). The a) adsorption and desorption curves at 77K and b) Brunauer-Emmett-Teller (BET) straight line of hexylamine treated sodium montmorillonite (NaM-HA).

The specific surface area of the NaM-HA sample was calculated from the following relationships

$$A / \text{m}^2 \text{g}^{-1} = (n_m / \text{mol g}^{-1}) \times (a_M / \text{m}^2) \times (N_A / \text{mol}^{-1}) \quad (3)$$

$$A / \text{m}^2 \text{g}^{-1} = 97524 (n_m / \text{mol g}^{-1}) \quad (4)$$

where the area occupied by an N_2 molecule and the Avogadro constant were respectively $a_M = 1.6 \times 10^{-20}$ and $N_A = 6.02 \times 10^{23}$. The calculated value of A was $71 \text{ m}^2 \text{g}^{-1}$. Since it was known that the value of A was $43 \text{ m}^2 \text{g}^{-1}$ for NaM it was apparent that the adsorption of HA increased the A value 65 %. The value of the overall heat of adsorption (q) was calculated as follows from the relationship between the other BET constant c and q :

$$q = RT \ln c \quad (5)$$

$$q = 8.314 \times 77 \ln 31 = 2198 \text{ J mol}^{-1}$$

Since this heat flows from the system to the environment during the adsorption, the enthalpy of adsorption was $\Delta H = -2198 \text{ J mol}^{-1}$. The fact that the exothermic adsorption heat was rather small showed that N_2 was adsorbed physically on NaM-HA. For the facility of adsorption and desorption calculations, it was assumed that the pores inside the solid were cylindrical. As the relative equilibrium pressure increased up to $x = 0.35$, all the mesopores that had radii (r) smaller than 1 nm were filled and the surfaces of the mesopores that had radii in the interval, $1 \text{ nm} < r < 25 \text{ nm}$, were covered multimolecularly. As the relative equilibrium pressure increased in the interval $0.35 < x < 0.96$ first, the smaller then, the larger mesopores that were covered multimolecularly were filled by capillary condensation. As the relative equilibrium pressure increased in the interval $0.96 < x < 1$, the macropores that had r values greater than 25 nm were filled. At $x=1$, bulk liquid nitrogen was discharged. From then on, desorption began. In the interval $0.96 < x < 1$, the liquid nitrogen volumes expressed as adsorption capacities (V) were calculated from the desorption data. In the same interval, the mesopore volumes were calculated from the following corrected Kelvin equation³⁴.

$$r / \text{nm} = 0.952 / \ln x + 0.735 / (\ln x)^{1/3} \quad (6)$$

The V - r mesopore size distribution curve plotted by the calculated values are shown in Fig. (7). The specific micropore-mesopore volume corresponding to $r = 25 \text{ nm}$ was read from the graph as $V = 0.229 \text{ cm}^3 \text{g}^{-1}$ and its value corresponding to $r = 1 \text{ nm}$ was $V_{mi} = 0.067 \text{ cm}^3 \text{g}^{-1}$. The specific mesopore volume which is the difference between these two values was calculated as $V_{me} = 0.162 \text{ cm}^3 \text{g}^{-1}$. Since the value of V was 0.104, it was understood that the adsorption of HA produced an increase of 120 % in pore volume.

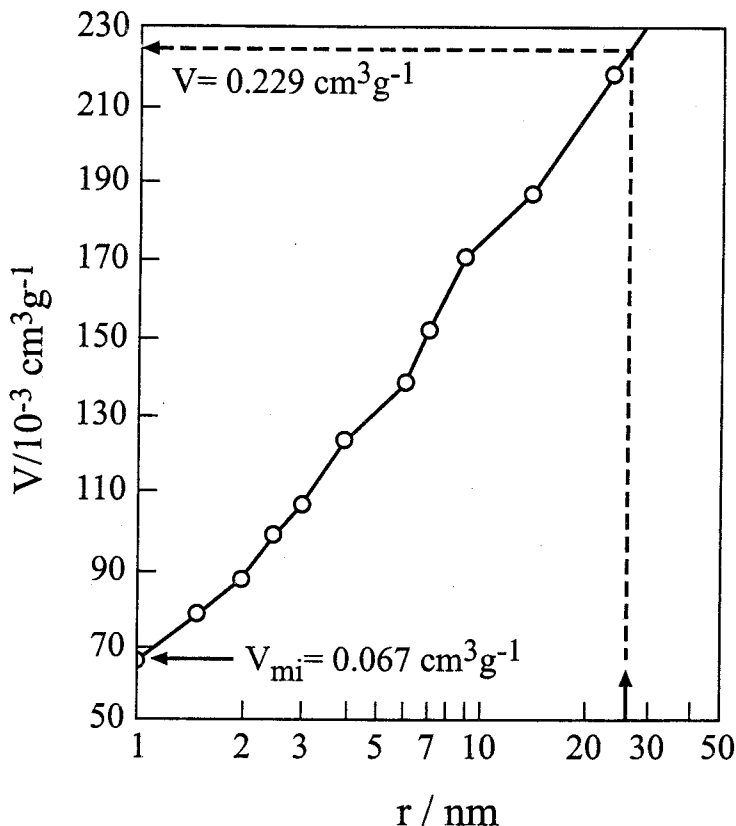


Fig. (7). The mesopore size distribution curve of hexylamine treated sodium montmorillonite (NaM-HA).

CONCLUSION

It was understood that the distance between the 2:1 layers of NaM was enlarged by the adsorption of HA. By comparing of the magnitudes of the HA molecule and the enlargement it was decided that HA had entered horizontally between the 2:1 layers and was adsorbed. It is thought that a chelation took place between the octet vacancies and the unshared electron pair on the nitrogen of the amine. It was understood that the pore structure of NaM was ameliorated by the adsorption of HA.

ACKNOWLEDGEMENT

The authors thank the Scientific and Technical Research Council of Turkey for supporting this work by the project TBAG-1986 (100T101).

REFERENCES

1. Grim, R. E.; Güven, N. *Bentonites, Geology, Mineralogy, Properties, and Uses, Developments in Sedimentology, Volume 24*, Elsevier, Amsterdam, 1978.
2. Murray, H. H. *Clay Miner.* 1999, 34, 39.
3. Grim, R. E. *Clay Mineralogy*, 2 nd ed., McGraw-Hill, New York 1968.
4. Grim, R. E. *Clays Clay Miner.* 1988, 36, 97.
5. Lermut, A. R.; Lagaly, G. *Clays Clay Miner.* 2001, 49, 393.
6. Luchham, P. F.; Rossi, S. *Adv. Colloid Intf. Sci.* 1999, 82, 43.
7. Dimov, V. I.; Ilieva, A. W. *Clays Clay Miner.* 2000, 48, 1.
8. Falares, D.; Lezon, F. *Clays Clay Miner.* 2000, 48, 549.
9. Adams, J. M. *Appl. Clay Sci.* 1987, 2, 309.
10. Lagaly, G. *Philos. T. Roy. Soc. A.* 1984, 1311, 315.
11. Breen, C.; Watson, R.; Madejeva, J.; Komadel, P.; Klapysa, Z. *Langmuir*, 1997, 13, 6473.
12. Sheng, G.; Boyd, S. A. *Clays Clay Miner.* 2000, 48, 43.
13. Wolfe, T. A.; Demirel, T.; Baumann, E. R. *Clays Clay Miner.* 1885, 33, 301.
14. Kovalska, M.; Güler, H.; Cocks, D. L. *Sci Total Environ.* 1994, 141, 223.
15. Falares, P.; Kovanis, I.; Lezou, F.; Seiragakis, G. *Clays Clay Miner.* 1999, 34, 221.
16. Takashima, M.; Sano, S.; Ohara, S. J. *Imaging Sci. Techn.* 1993, 37, 163.
17. Bolgar, R. *Ind. Miner.* 1995, August, 57.
18. Gamiz, E.; Linares, J.; Delgado, R. *Appl. Clay Sci.* 1992, 6, 359.
19. Barrer, R. M. *Clays Clay Miner.* 1989, 37, 385.
20. Pusine, A.; Braschi, I.; Gessa, C. *Clays Clay Miner.* 2000, 48, 19.
21. Yalçın, H.; Gümüşer, G. *Clay Miner.* 2000, 35, 807.
22. Onal, M.; Sarıkaya, Y.; Alemdaroğlu, T. *Turk. J. Chem.* 2001, 25, 241.
23. Onal, M.; Sarıkaya, Y.; Alemdaroğlu, T.; Bozdoğan, İ. *Clays Clay Miner. Baskıda.*
24. Sarıkaya, Y.; Aybar, S. *Commun. Fac. Sci. Uni. Ank.* 1978, B24, 33.
25. Moore, D. M.; Reynolds, R. C. *X-Ray Diffraction and the Identification and Analysis of Clay Minerals*, 2 nd ed. , Oxford University Press, Oxford, 1987.
26. Chipera, S. J.; Bish, D. L. *Clays Clay Miner.* 2001, 49, 398.
27. Madajeva, J.; Komadel, P. *Clays Clay Miner.* 2001, 49, 410.
28. Erdik, E. *Organik Kimyada Spektroskopik Yöntemler*, Gazi Büro Kitabevi, 1993, pp. 118-139.
29. Silverstein, R. M.; Bassler, G. C.; Morrill, T. C. *Spectrometric Identification of Organic Compounds*, 4 th ed., John Wiley, New York, 1981, pp. 168-172.

30. Guggenheim, S.; Gross, A. F. K. *Clays Clay Miner.* 2001, 49, 433.
31. Sarıkaya, Y.; Onal, M.; Alemdaroğlu, T.; Bozdoğan, İ. *Clays Clay Miner.* 2000, 48, 557.
32. Coats, A.; Redfern, J. P. *Nature*, 1964, 201, 68.
33. Brunauer, S.; Emmett, P. H.; Teller, E. J. *Am. Chem. Soc.* 1938, 60, 309.
34. Gregg, S. J.; Sing, K. S. W. *Adsorption, Surface Area and Porosity*, 2 nd ed., Academic Press, London, 1982.